

STUDY OF INFLUENCE OF BUILDUP FACTOR FORM ON SIMULATED RADIOGRAPHIC IMAGE

by

Predrag MARINKOVIĆ

Received on January 12, 2009; accepted in revised form on January 29, 2009

The objective of the study presented in this paper is the analysis of influence of different buildup factor forms on a simulated radiographic image. Simulated radiographic images are obtained by means of the ray-tracing technique. Scattered photons are modelled using the generally accepted geometric progression form, linear form and tabulated data of buildup factors. Simulated images were compared to the reference results obtained by Monte Carlo calculation. The best agreement to Monte Carlo simulated images is achieved for the geometric progression form of buildup factor.

Key words: simulation of radiographic image, Monte Carlo, buildup factor, ray-tracing

INTRODUCTION

Simulation offers powerful means of choosing the most suitable components and of predicting the future device performance, by acting as a virtual experimental worktable. Radiographic images can be obtained by simulation in short time and at low cost and may enable the behaviour of the whole imaging system to be investigated in complex situations. It can also be a precious tool to study the ability to detect small lesions, depending on their size and position in the object of imaging (a patient body). Simulation can be useful, when developing any specific imaging setup, in choosing the best components, optimizing the imaging parameters and saving time by reducing the number of experimental tests. Simulation also presents an important potential for testing the performance of image processing procedures in a virtual environment, where all parameters are fully controlled. In contrast to an experiment, simulation provides the

capability of examining each aspect of the imaging process separately. It can be used to interpret complex studies by comparing them to the corresponding simulation results. Simulation can be also used as a didactic tool for training physicians and medical technicians.

Radiation transport modelling methods used in the radiography simulation fall into one of two broad categories: stochastic (Monte Carlo) and deterministic. Monte Carlo (MC) methods are typically the tool of choice for simulating X-ray image formation, but deterministic methods offer potential advantages in computational efficiency for many complex imaging problems.

MC methods allow the user to study the complete physics of radiography (*e. g.* coherent and incoherent scattering, fluorescence, bremsstrahlung, and annihilation), which cannot be effectively simulated by deterministic models [1, 2]. Their major drawback is the huge time required for execution on a single processor computer.

For practical research and clinical application deterministic models are more appropriate. Among them, ray-tracing methods and analytical models are mostly used [3, 4]. They have less calculation burden than MC and have no problem with statistics, so that the fast simulation of transmission images can be established. Photon scattering and reflection in medical imaging energy domain can be successfully treated by deterministic methods [5, 6].

The combined deterministic method and MC method, known as a hybrid simulation of the radiographic process, is proposed too [7, 8]. The advantage

Nuclear Technology & Radiation Protection
Scientific paper
UDC: 539.122:519.245
BIBLID: 0451-3994, 24 (2009), 1, pp. 38-45
DOI: 10.2298/NTRP0901038M

Author's address:
Faculty of Electrical Engineering
Belgrade University
73, Bulevar Kralja Aleksandra
P. O. Box 35-54, 11120 Belgrade, Serbia

Author's e-mail:
marinkovic@etf.bg.ac.rs

of complementarities between deterministic and stochastic approach is used.

In this paper, the ray-tracing method with the exposure dose buildup factor is applied to the simulation of a radiographic image. The influence of different buildup factor forms on the image quality is studied.

MODEL

The process of the simulation of a radiographic image can be divided into four steps: the X-ray beam generation, beam interaction with material, determination of material chemical composition, and conversion of the exposure dose to optical density in the imaging detector.

The source of X-rays is a radiological tube. The spectral distribution of emitted photons is an important property of an X-ray beam. Beside measurements, several computer codes have been proposed to determine photons spectrum [9]. The computer code XCOMP5R is used in all calculations presented in this paper [10]. It allows the calculation of the spectrum in energy groups (bends) that have width of 0.5 keV or 1 keV.

In particle transport physics, ray-tracing is a method for calculating the particle path through a system with regions of varying absorption and scatter characteristics. The ray-tracing method together with the X-ray attenuation law are the basis of the method described in this paper.

The influence of buildup factor forms on a simulated radiographic image is the objective of the study in this paper. The exposure dose of photons' buildup factors for point isotropic sources in an infinite homogenous media is usually used in a radiation protection analysis as a part of the point-kernel method. They are always useful for practical calculations in a gamma-ray shield design. Problems concerning the deep penetration of photons through the matter can be successfully treated by means of buildup factors. These factors are available for up to 40 mean free paths (mfp) and are referred to as ANS/ANSI-6.4.3 standard [11]. These data have been developed for a large number of elements, but include only three compounds or mixtures (water, concrete, and air). The materials not included in the standard data must be treated separately [12].

Buildup factors generally depend on the source and shield geometry. The use of buildup factors for point isotropic sources is almost always conservative [13], *i. e.* the estimated dose is greater than the one for the finite medium.

Tabulated values of buildup factors can be found in a number of sources. After that, buildup factors are interpolated or extrapolated by means of an approximation method in order to speed-up the calculation. Although some analysts prefer to use tables taken directly from the computer code, others prefer the ana-

lytical (functional) forms of buildup factors. The functional forms, among others, include linear, polynomial (quadratic), Taylor [14], Berger [14], and Harima [15] formulae. The Harima formula, as an approach of very high accuracy, is well known as geometric progression (G-P) form of the buildup factor.

There is a number of analytical expressions that have been used to represent the buildup factor B . Among the most popular were expressions known as Taylor's form or Berger form of the buildup factor. These types of buildup factors are not applicable to radiographic imaging studies because they do not cover the energy range of interest. For the state-of-the-art buildup factor data, extended up to lower photon energies and deeper penetrating length, the accuracy of these forms is not acceptable for a low- Z materials and low energies.

Among simple buildup factor forms, the well known linear form

$$B(E, \hat{x}) = 1 + k\hat{x} \quad (1)$$

is used in this study. The parameter k is often taken as a constant (*e. g.*, 0.3 to 1), but actually varies significantly with thickness and photon energy, and \hat{x} is the distance in mean free paths. In this paper the value of k is selected to be 0.9.

It is clear now that the best available form of the buildup factor is the G-P formula [15]. The G-P formula, for photon energies ranging between 15 keV and 15 MeV, is expressed as

$$B(E, \hat{x}) = \begin{cases} 1 + (b - 1)(K^{\hat{x}} - 1)/(K - 1), & \text{for } K \neq 1 \\ 1 + (b - 1)\hat{x}, & \text{for } K = 1 \end{cases} \quad (2)$$

$$K(\hat{x}) = c\hat{x}^a + d \frac{\tanh(\hat{x}/X_k - 2) - \tanh(-2)}{1 - \tanh(-2)} \quad (3)$$

where \hat{x} is the source-detector distance in mean free paths, b is the value of the buildup factor at one mean free path, and K is the multiplication per mean free path. The parameters a , c , d , and X_k are fitting values which depend on the photon energy from the source. The G-P form of the buildup factor is the favoured choice because the buildup factors decrease for large distances and do not increase exponentially as it occurred in the Berger form. It has a wider range of applicability as compared to the linear, Berger or Taylor form.

The coefficients for the G-P buildup factor for water that are used in calculations are presented in tab. 1. Fitting function parameters for 22 materials (elements and only three compounds and mixtures) are utilized in the form of data files incorporated in ANS-6.4.3 standards.

The tabulated values of buildup factors [17], used in this study, are presented in tab. 2.

Table 1. G-P parameters for water [16]

E [keV]	b	c	a	X_k	d
15	1.188	0.464	0.172	14.00	-0.0829
20	1.449	0.532	0.152	14.61	-0.0764
30	2.411	0.741	0.084	14.62	-0.0452
40	3.587	1.114	-0.018	12.48	0.0013
50	4.554	1.457	-0.084	13.69	0.0341
60	5.018	1.735	-0.127	13.70	0.0676
80	5.030	2.054	-0.167	13.84	0.0763
100	4.627	2.207	-0.184	13.27	0.0799
150	3.888	2.206	-0.180	14.27	0.0738

Table 2. Tabulated values of exposure dose buildup factor (with bremsstrahlung) for water

mfp	E [keV]									
	15	20	30	40	50	60	80	100	150	
0.5	1.11	1.25	1.69	2.18	2.51	2.65	2.57	2.38	2.07	
1	1.17	1.41	2.25	3.41	4.40	4.93	4.98	4.57	3.76	
2	1.26	1.64	3.20	6.02	9.12	11.4	12.6	11.8	9.41	
3	1.32	1.81	4.04	8.81	15.0	20.2	24.4	23.6	18.9	
4	1.36	1.95	4.80	11.7	21.9	31.5	40.8	40.8	33.0	
5	1.40	2.07	5.25	14.8	29.8	45.3	62.5	64.3	52.8	
6	1.44	2.18	6.21	18.0	38.7	61.7	90	95.1	79.1	
7	1.47	2.27	6.88	21.3	48.6	80.9	124	134	113	
8	1.49	2.36	7.53	24.8	59.5	103	165	183	156	
10	1.54	2.52	8.79	32.1	84.8	157	273	314	272	

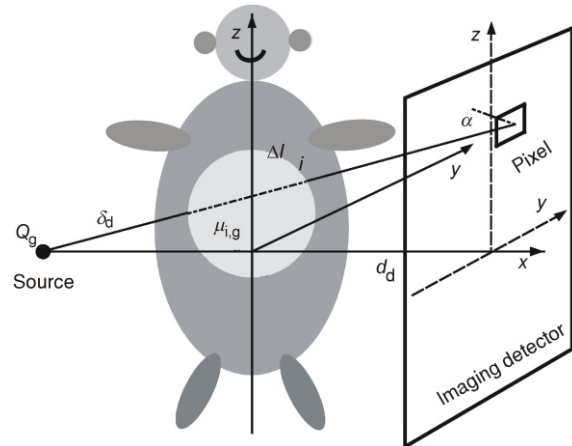
The basic assumption incorporated in the model used in this study with respect to the buildup factor is the application of a single medium (water) buildup factor for heterogeneous media. This assumption is based on the knowledge that human body consists mainly of water.

The computer code XIMRAD is developed based on the model using the ray-tracing method together with the X-ray attenuation law. A single beam of photons is emitted from the point source towards every pixel centre of the imaging detector. Each beam may intersect a certain number of meshes on the sample surface or at the interfaces between different parts of the imaging object (fig. 1).

The exposure dose $D_{X,d}$ with the buildup factor in a pixel of the detector from a beam of X-rays is

$$D_{X,d} = \frac{q_e}{w_j} \sum_g B(E_g, \sum_i \mu_{i,g} \Delta l_i) E_g \frac{\mu_{en,g}^{air}}{\rho_{air}} \frac{Q_g}{4\pi\delta_d^2} e^{-\mu_{i,g} \Delta l_i} \cos \alpha \quad (4)$$

where E_g is the energy of photons in the energy group g , $q_e = 1.6 \cdot 10^{-19} C$ and $w_j = 34 eV$ is the energy of the ionization of air. The value $\mu_{en,g}^{air}$ is the air energy absorption coefficient in the energy group g , ρ_{air} is the

**Figure 1. Model geometry**

density of air, Q_g is the source intensity, and $B(E_g, \sum_i \mu_{i,g} \Delta l_i)$ is the exposure dose buildup factor. The value $\cos \alpha = d_d / \delta_d$, where d_d is a normal distance between the imaging detector and the source and δ_d is the distance from the pixel centre to the source.

The processes of photon detection in imaging detectors are habitually modelled in two steps. In the first step, the energy deposited in the material of the detector is determined. The second one, specific to each type of a detector, treats the physical phenomena involved in the photon energy absorption transformation to measuring quantity. In this paper, the exposure dose of radiation in an imaging detector is considered only.

Beside the geometry and material composition of the imaging object, the size, position and number of pixels of the imaging detector can be selected in the computer code input. The position and spectrum of the photon source, geometry arrangement of the setup source-imaging object-detector are also defined in the computer code input.

MODEL VALIDATION

In order to study the buildup factor form the influence on the radiographic image quality, a series of numerical experiments was performed. In fig. 2, the radiographic setup (phantom) used in this study is shown. It is formed by means of the simple geometry (SG) model. The objects are described by closed surfaces separating regions of homogenous material. Several objects can be arranged in a virtual scene combined by simple Boolean operators forming complex parts.

The phantom is a water filled cylinder with eight spheres of different materials and different radii. For the phantom outside surface, a cylinder defined by means of surface equations $(x/a)^2 + (y/b)^2 = 1$, $z = H/2$, and $z = -H/2$, where $a = 5$ cm, $b = 20$ cm, and $H = 44$ cm is

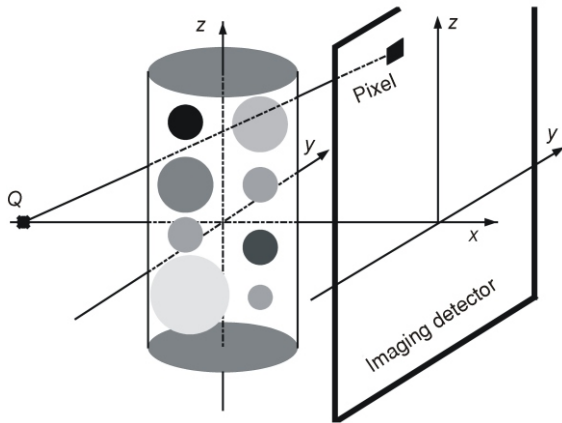


Figure 2. Phantom

chosen. Materials, the compositions of which is taken from ICRU-44 Report [18], and the location of the spheres' centres (x_C, y_C, z_C) and spheres' radii are given in tab. 3.

Table 3. Parameters of spheres

i	$x_{C,i}$	$y_{C,i}$	$z_{C,i}$	R_i	Material
1	0	-7	11	1.5	Bone cortical (ICRU-44)
2	0	-7	6	1.5	Air
3	0	-7	0	4.0	Adipose tissue (ICRU-44)
4	0	-7	-11	1.5	Muscle skeletal
5	0	7	10	1.5	Breast tissue (ICRU-44)
6	0	7	0	4.0	Soft tissue (ICRU-44)
7	0	7	-6	1.5	B-100 bone equivalent plastic
8	0	7	-11	1.5	Lung tissue (ICRU-44)

A single point source, which emits $Q = 1 \cdot 10^9$ photons, was located at $x_Q = -100$ cm, $y_Q = 0$, and $z_Q = 0$. In the first case of this study, the anode tube voltage was 60 kV and the anode material was tungsten. The spectrum of the emitted photons after filtration through 3.5 mm thick aluminum is shown in fig. 3. In the second case of the study, the anode tube voltage was 80 kV. The spectrum of the emitted photons after filtration through 3 mm thick aluminum is shown in fig. 3. In the third case of the study, the anode tube voltage was 120 kV and the spectrum of emitted photons after filtration through 12 mm thick aluminum is shown in fig. 3. In all cases the anode material was tungsten (W).

The imaging detector located 10 cm from the centre of the phantom was divided into 310 340 pixels (each size $0.1 \cdot 0.1$ mm²).

As buildup factors are calculated for the infinite medium, with the source and detector inside the material, a correction for the finite medium must be done. In fig. 4, the correction diagram can be seen, which is obtained by MCNP5 simulation [19] and relates buildup in the finite and infinite medium ratio (B_{MC}/B_{G-P}) and the energy of photons. For this purpose, the imaging

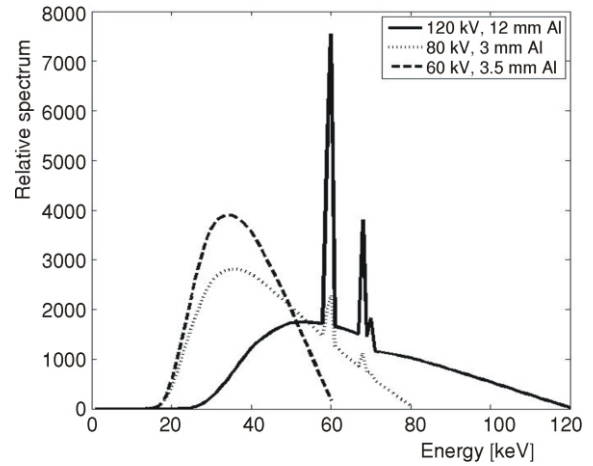


Figure 3. Spectra of X-photons emitted from X-ray tube at distance 1 m from tungsten anode. Photons are filtered through aluminum filter. Angle was 17° for all cases

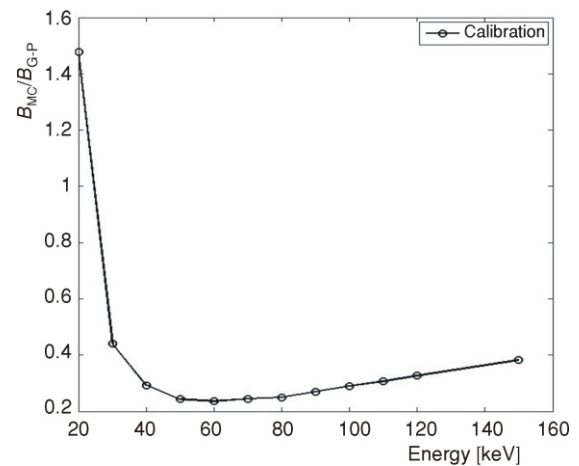


Figure 4. Ratio of buildup in finite and infinite medium (B_{MC}/B_{G-P}) as a function of photon energy

object is replaced by a water cylinder of the equivalent thickness and radius, keeping other simulation conditions unchanged. For low energies, the ratio B_{MC}/B_{G-P} is greater than one because in the finite medium and with the detector outside the medium, the scattered low energy photons in air are not absorbed significantly as in the medium.

Figure 5 shows the images of the exposure dose of the total (direct plus scattered) radiation in the detector in the case of the 60 kV X-ray tube anode voltage. In that figure, the image for G-P form of the buildup factor and the image obtained by MC simulation can be seen.

The comparison of the simulated images (for different forms of buildup factors and MC simulation) is shown in fig. 6 where the profiles of doses of the total photons can be seen, corresponding to the 85th column of the images from fig. 5 and the images for tabulated

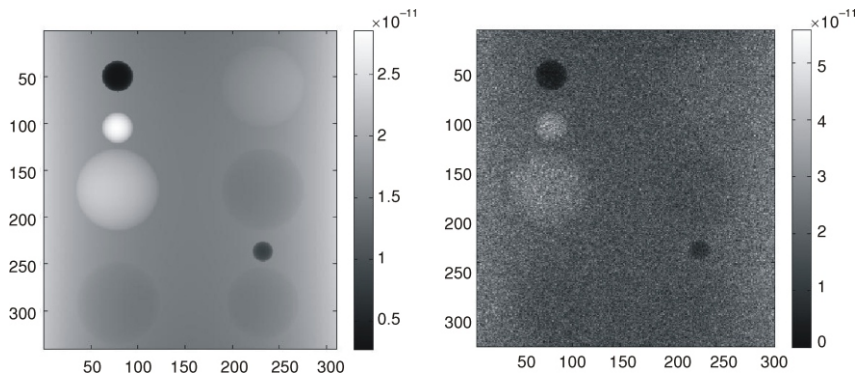


Figure 5. Simulated radiographic images for G-P form of buildup factor (left) and MC simulation (right) for 60 kV tube anode voltage

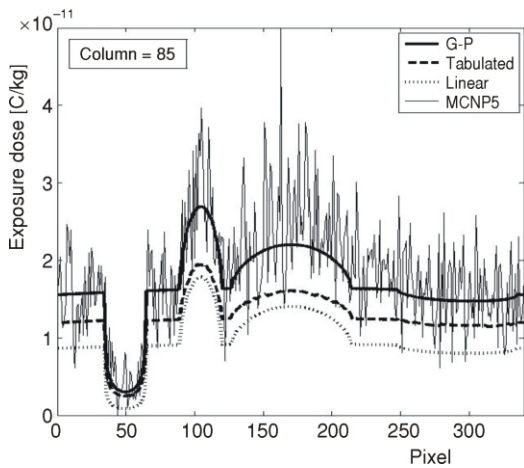


Figure 6. Exposure dose distributions obtained by different forms of buildup factors and MC simulation for 85th column of pixels in case of 60 kV

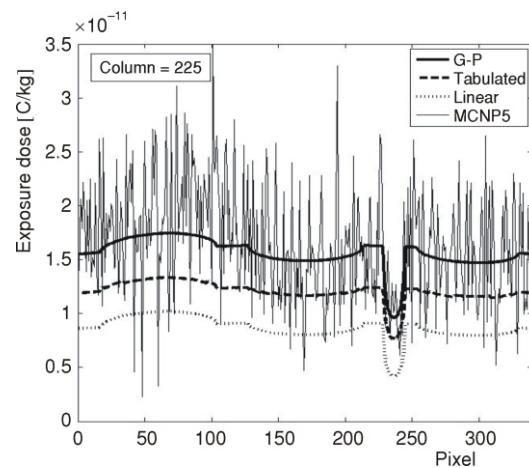


Figure 7. Exposure dose distributions obtained by different forms of buildup factors and MC simulation for 225th column of pixels in case of 60 kV

data and linear form of the buildup factor (not shown in the paper).

In fig. 7 profiles of the doses of the total photons can be seen, corresponding to the 225th column of the images from fig. 5 and the images for tabulated data and linear form of the buildup factor.

From the foregoing figures, it can be noticed that good agreement to MC results can be achieved in the case of G-P form of the buildup factor. The tabulated data results and the linear form of the buildup factor are a bit below the values of the MC results.

Figure 8 shows the images of the exposure dose of the total radiation in the imaging detector in the case

of the 80 kV X-ray tube anode voltage, tungsten anode material, and the 3 mm thick aluminum filter.

The comparison of the simulated images is shown in fig. 9 where the profiles of doses of the total photons can be seen, corresponding to the 85th row of images from fig. 8, and the images for the tabulated data and the linear form of the buildup factor.

In fig. 10, the profiles of the doses of the total photons can be seen, corresponding to the 225th column of images from fig. 8 and the images for the tabulated data, and the linear form of the buildup factor.

In the case of the 80 kV tube voltage the best results are obtained for the G-P form of the buildup fac-

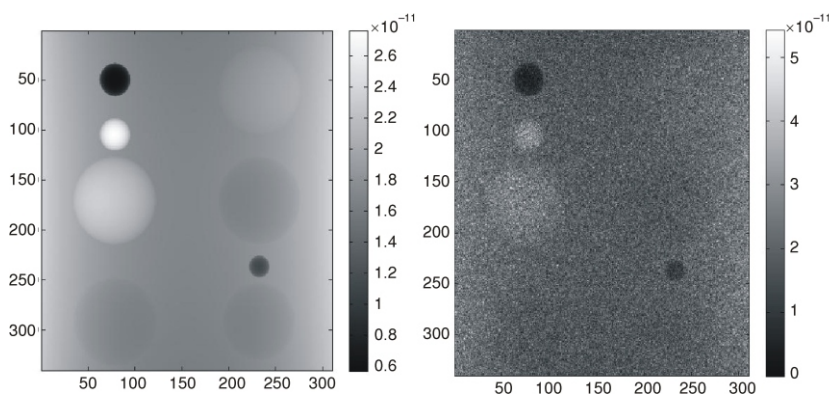


Figure 8. Simulated radiographic images for 80 kV tube anode voltage and G-P form of buildup factor (left) and MC simulation (right)

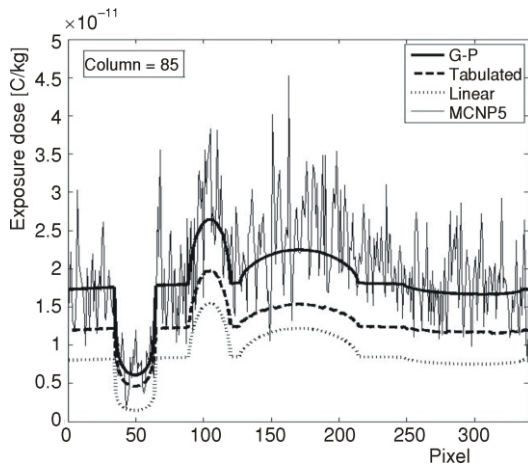


Figure 9. Exposure dose distributions obtained by different forms of buildup factors and MC simulation for 85th column of pixels in case of 80 kV

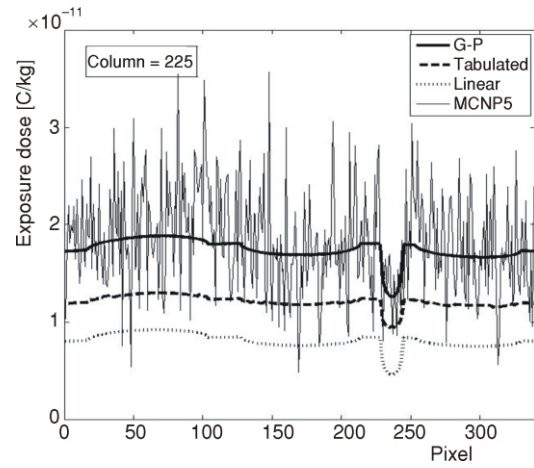


Figure 10. Exposure dose distributions obtained by different forms of buildup factors and MC simulation for 225th column of pixels in case of 80 kV

tor, again. The results for the linear form and tabulated data are below the values of MC results significantly.

Finally, fig. 11 shows the images of the exposure dose of the total radiation in the imaging detector in the case of the 120 kV X-ray tube anode voltage, tungsten anode material, and the 12 mm thick aluminum filter.

The comparison of the simulated images is shown in fig. 12 where the profiles of the doses of the total photons can be seen, corresponding to the 85th row of images from fig. 11 and the images for the tabulated data and the linear form of the buildup factor.

In fig. 13 the profiles of the doses of the total photons can be seen, corresponding to the 225th col-

Figure 11. Simulated radiographic images for 120 kV tube anode voltage and G-P form of buildup factor (left) and MC simulation (right)

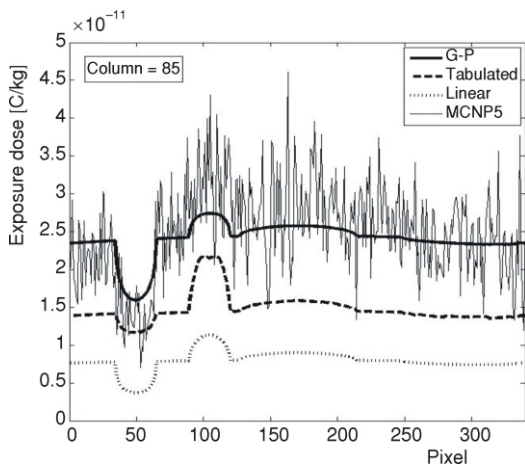
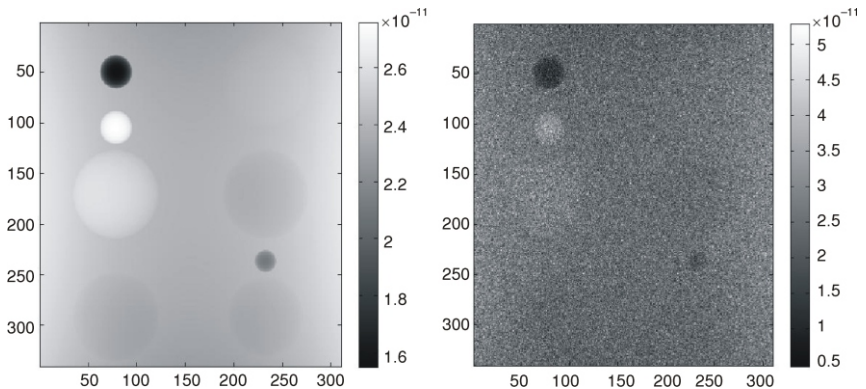


Figure 12. Exposure dose distributions obtained by different forms of buildup factors and MC simulation for 85th column of pixels in case of 120 kV

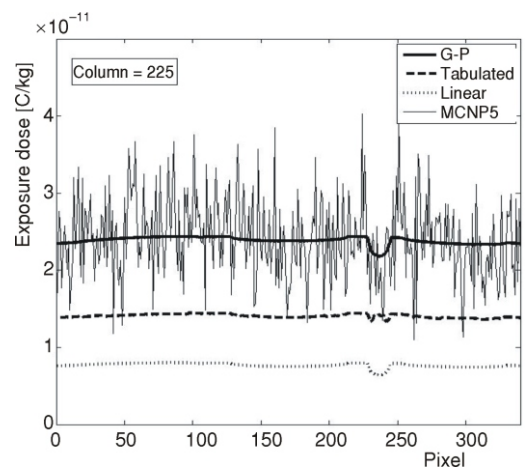


Figure 13. Exposure dose distributions obtained by different forms of buildup factors and MC simulation for 225th column of pixels in case of 120 kV

umn of images from fig. 11 and the images for the tabulated data and the linear form of the buildup factor.

In the case of the 120 kV tube voltage the best results are obtained for G-P form of the buildup factor, again. The results for the linear form and the tabulated data are below the values of MC results significantly.

The expected reduction of the image contrast with the increase of the beam energy can be seen in the figures that show the distributions of the exposure dose.

CONCLUSIONS

In this paper a simple and flexible tool is proposed for simulation of radiographic image, and a computer code, based on this method, is written. By means of the developed computer code, the influence of different parameters on the image quality is investigated. This approach is considerably faster than probabilistic methods and therefore requires short computational time on a single processor PC.

The comparison of results achieved by the proposed ray-tracing method with G-P for the buildup factor to the reference results obtained by MCNP5 code shows full agreement of the simulated images for the energies of X-photons usually used in general radiography.

ACKNOWLEDGEMENT

This work is supported by the Ministry of Science and Technological Development, Republic of Serbia, under a grant to the Faculty of Electrical Engineering, Belgrade University, Belgrade, Republic of Serbia 451-03-516/2006-01/141041G. The author is grateful to M. Pešić from the Vinča Institute of Nuclear Sciences in Belgrade for the results obtained by the MCNP5 code.

REFERENCES

- [1] Winslow, M., Xu, X. G., Huda, W., Ogden, K. M., Scalzetti, E. M., Monte Carlo Simulation of Patient X-ray Images, *Am. Nucl. Soc. Trans.*, 90 (2004), pp. 459-460
- [2] Lazos, D., Kolitsi, Z., Pallikarakis, N., A Software Data Generator for Radiographic Imaging Investigations, *IEEE Trans. Informat. Technol. Biomed.*, 4 (2000), 1, pp. 76-79
- [3] Duvauchelle, P., Freud, N., Kaftandjian, V., Babot, D., A Computer Code to Simulate X-Ray Imaging Techniques, *Nucl. Instr. and Meth.*, B170 (2000), 1-2, pp. 245-258
- [4] Gliere, A., SINDBAD: from CAD Model to Synthetic Radiographs, in: Review of Progress in Quantitative Nondestructive Evaluation (Eds. D. O. Thomson, D. E. Chimenti), Vol. 17A, Plenum Publishing Co., Bristol and Philadelphia, USA, 1998
- [5] Ljubenov, V., Simović, R., Marković, S., Ilić, R. D., Photon Scattering and Reflection in Medical Diagnostic Energy Domain, *Nuclear Technology & Radiation Protection*, 23 (2008), 1, pp. 31-36
- [6] Marinković, P., Ilić, R., Spaić, R., A 3-D Point-Kernel Multiple Scatter Model for Parallel-Beam SPECT Based on a Gamma-Ray Buildup Factor, *Phys. In Med. and Biol.* 52 (2007), 19, pp. 5785-5802, DOI:10.1088/0031-9155/52/19/004
- [7] Freud, N., Létang, J.-M., Babot, D., A Hybrid Approach to Simulate Multiple Photon Scattering in X-Ray Imaging, *Nucl. Inst. and Meth. in Phys. Res.*, B227 (2005), 2, pp. 551-558
- [8] Tabary, J., Guillemaud, R., Mathy, F., Gliere, A., Hugonnard, P., Combination of High Resolution Analytically Computed Uncollided Flux Images with Low Resolution Monte Carlo Computed Scattered Flux Images, *IEEE Trans. Nucl. Eng.* 51 (2004), 1, pp. 212-217
- [9] Meyer, P., Buffard, E., Mertz, L., Kennel, C., Constantinesco, A., Siffert, P., Evaluation of the Use of Six Diagnostic X-Ray Spectra Computer Codes, *The British Journal of Radiology*, 77 (2004), pp. 224-230
- [10] Nowotny, R., Höfer, A., Ein Programm für die Berechnung von diagnostischen Röntgenspektren, *Fortschr. Röoetgenstr.*, 142 (1985), pp. 685-689
- [11] ***, ANS-6.4.3 Standard Reference Data, NUREG/CR-5740, ORNL/RSIC-49/R1, 1991
- [12] Sakamoto, V., Tanaka, S., Interpolation of Gamma-Ray Buildup Factors for Point Isotropic Source with Respect to Atomic Number, *Nuc. Sci. and Eng.*, 100 (1988), 1, pp. 33-42
- [13] Shultis, J. K., Faw, R. E., Radiation Shielding, American Nuclear Society, La Grange Park, IL, USA, 2000, ISBN 0-89448-456-7
- [14] Mashkovich, V. P., Protection for Ionizing Radiation, Handbook (in Russian), Atomizdat, Moscow, pp.137-140, 1982
- [15] Harima, Y., Sakamoto, Y., Tanaka, S., Kawai, M., Validity of the Geometrical Progression Formula in Approximating Gamma-Ray Buildup Factors, *Nucl. Sci. Eng.*, 94 (1986), 1, pp. 24-35
- [16] Trubey, D. K., Harima, Y., New Buildup Factor Data for Point Kernel Calculations, Technical Report, CONF-870405-10, DE87 000233, 1987
- [17] Shimizu, A., Onda, T., Sakamoto, Y., Calculation of Gamma-Ray Buildup Factors up to Depths of 100 mfp by the Method of Invariant Embedding, (III) Generation of an Improved Data Set, *J. of Nucl. Sci. and Tech.*, 41 (2004), 4, pp. 413-424
- [18] ***, Tissue Substitutes in Radiation Dosimetry and Measurement, ICRU Report 44 of the International Commission on Radiation Units and Measurements Bethesda, Md., USA, 1989
- [19] ***, X-5 Monte Carlo Team, MCNP-A General Monte Carlo N-Particle Transport Code, Version 5.1.1.2 - Vol. I-III, LANL, Los Alamos, April 2003

Предраг МАРИНКОВИЋ**СТУДИЈА УТИЦАЈА ОБЛИКА ФАКТОРА НАГОМИЛАВАЊА НА
СИМУЛИРАНУ РАДИОГРАФСКУ СЛИКУ**

Циљ студије приказане у овом раду је анализа утицаја различитих облика фактора нагомилавања на радиографску слику. Симулиране радиографске слике добијене су помоћу технике праћења зрака. Утицај расејаних фотона на слику процењен је помоћу фактора нагомилавања у виду општеприхваћене геометријске прогресије, линеарне форме и табелираних вредности. Симулиране слике упоређене су са референтним резултатима добијеним Монте Карло симулацијом. Најбоље слагање са референтним резултатима остварено је у случају примене облика фактора нагомилавања у виду геометријске прогресије.

Кључне речи: симулација радиографске слике, Монте Карло, фактор нагомилавања, праћење зрака
